Supplementary Information

Regulating Electric Double Layer Dynamics for Robust SEI in Fast-Charging Graphite Anodes

Jaeyeon Bang,[a] Seong-Soo Park,[b] Kyungjun Kim,[a] Hwiju Lee,[a] Ilyoung Choi,[c] Youngugk Kim,[c] JangHyuck Moon,[*b] Sang-Min Lee[*a,d]*

[a] Department of Battery Engineering, Graduate Institute of Ferrous & Eco Materials Technology (GIFT), Pohang University of Science and Technology (POSTECH), 77, Cheonam-Ro, Nam-Gu, Pohang, Gyungbuk 37673, Republic of Korea

[b] Department of Energy Systems Engineering, Chung-Ang University, 84 Heukseok-ro, Dongjak-gu, Seoul 06974, Republic of Korea

[c] Samsung SDI Co., Ltd. R&D Center, Suwon, 16678 Republic of Korea

[d] Department of Materials Science and Engineering, Pohang University of Science and Technology (POSTECH), 77, Cheonam-Ro, Nam-Gu, Pohang, Gyungbuk 37673, Republic of Korea

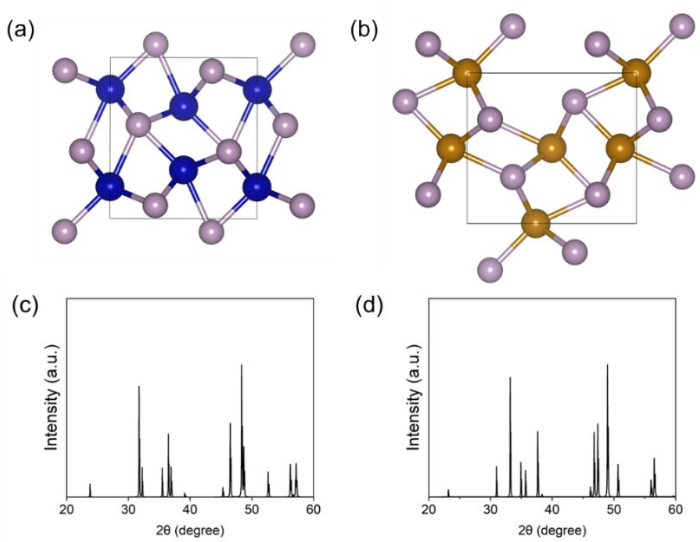

Fig. S1 Calculated crystal structures and XRD peaks of (a, c) CoP and (b, d) FeP, respectively.

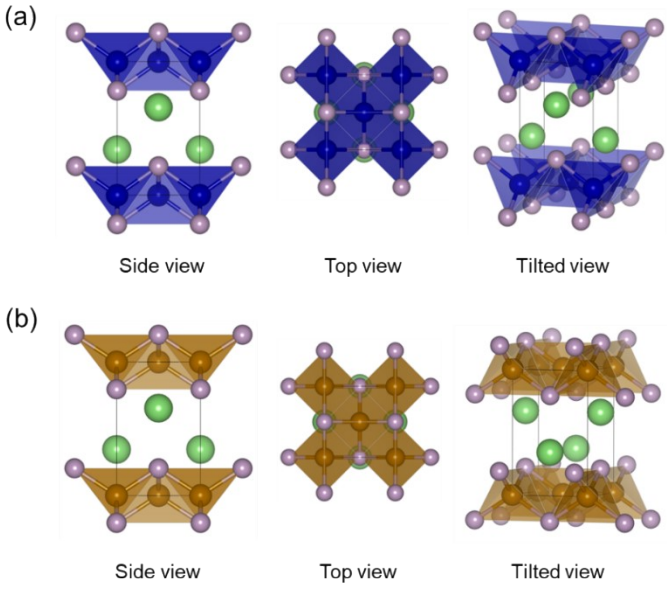

Fig. S2 Calculated crystal structures of (a) LiCoP and (b) LiFeP different viewing angles.

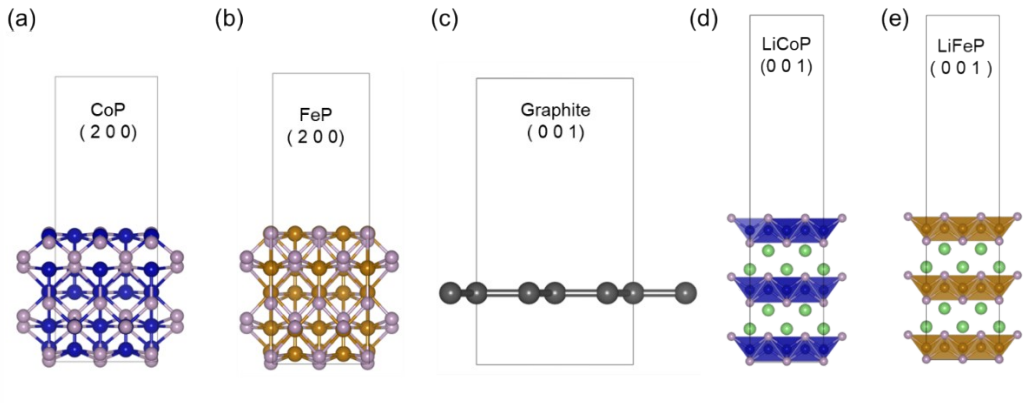

Fig. S3 The calculated surface of (a) (200) for CoP, (b) (200) for FeP, (c) (001) for graphite, (d) (001) for LiCoP, and (e) (001) LiFeP.

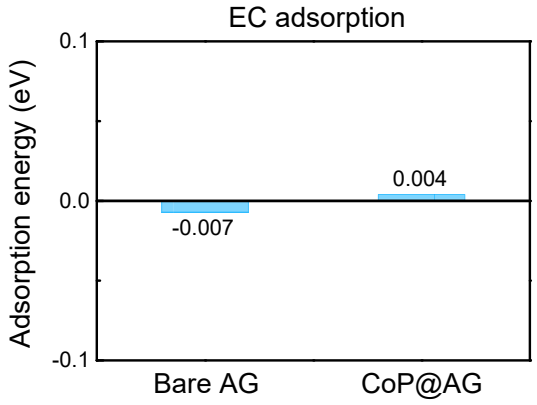

Fig. S4 Adsorption energy of EC for Bare AG and CoP@AG surface.

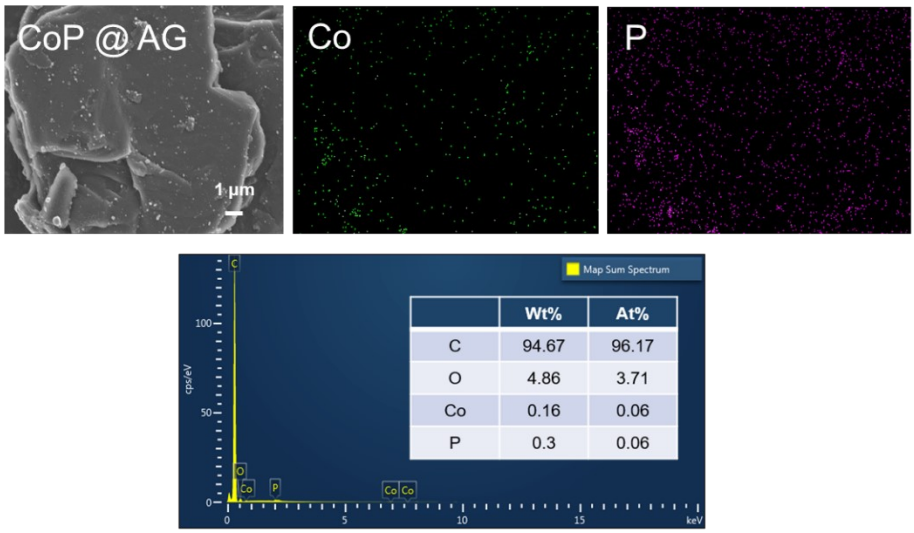

Fig. S5 Elemental distribution and composition ratio of CoP@AG

Sample	Element	Result	
CoP@AG	Co	0.45wt%	ICP-OES iCAP Pro
	P	0.3wt%	

Fig. S6 ICP-OES measurement of CoP@AG powder

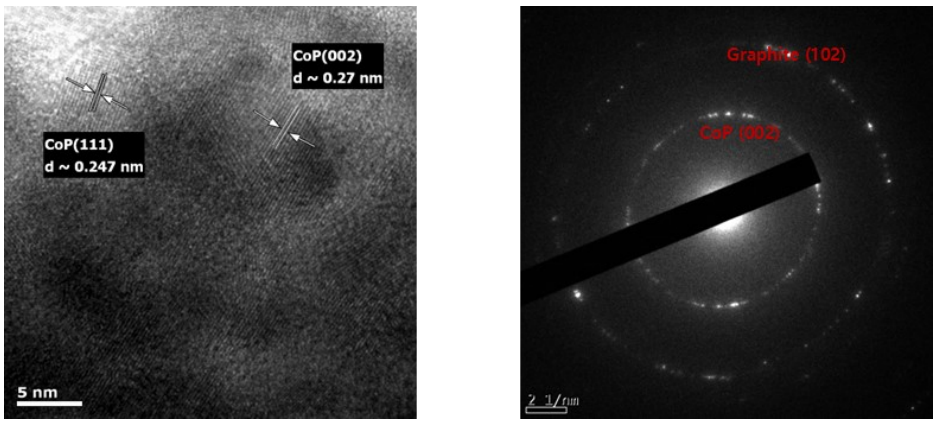

Fig. S7 TEM and SAED images of CoP@AG particles

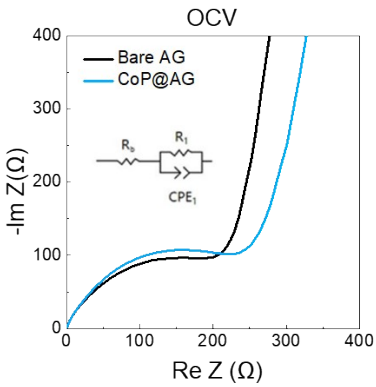

	R_b(Ω)	R_{ct}(Ω)
Bare AG	0.8	201.6
CoP@AG	0.8	235.8

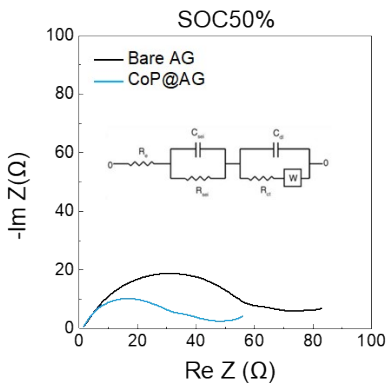

	R_b(Ω)	R_{SEI}(Ω)	R_{ct}(Ω)
Bare AG	0.8	**57.2**	**20.3**
CoP@AG	1.1	**29.4**	**16.6**

Fig. S8 Nyquist plots of Bare AG and CoP@AG half cells at OCV state and SOC 50% state.

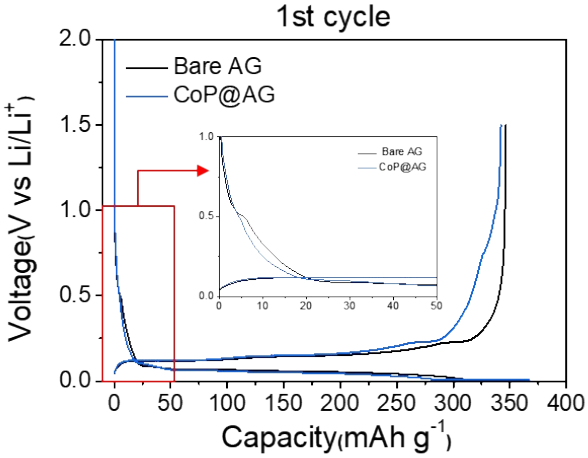

Fig. S9 Galvanostatic charge/discharge profiles of Bare AG and CoP@AG using electrolyte without FEC additive.

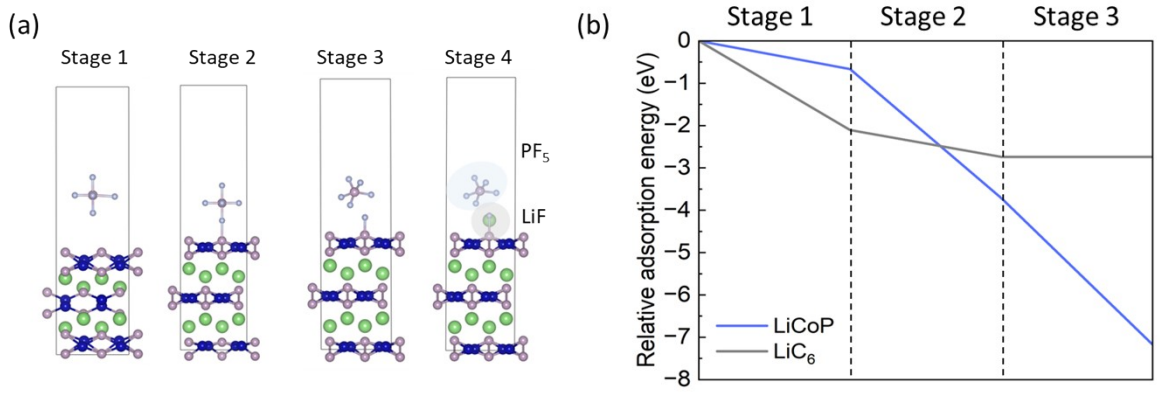

Fig. S10 (a) Decomposition process of PF_6^- and formation of LiF on LiCoP surfaces. (b) The relative adsorption(formation) energies of PF_6^- adsorption(Stage 2), PF_6^- decomposition(Stage 3) and LiF formation(Stage 3) on LiCoP and LiC_6 surface.

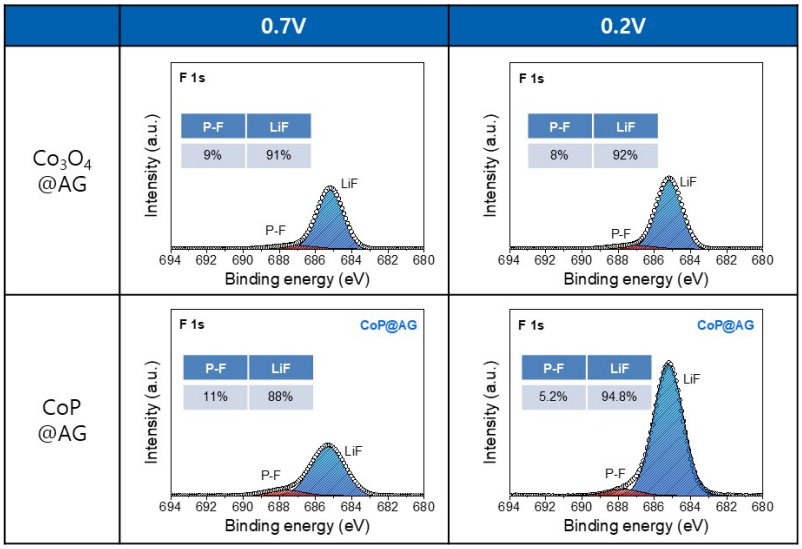

Fig. S11 Evolution behavior of the SEI layer of Co_3O_4@AG through XPS analysis after charging to 0.7V and 0.2V.

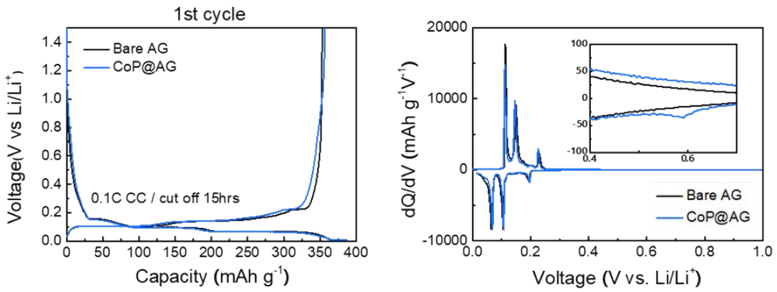

	Charge capacity	Discharge capacity
Bare AG	365.1 mAh g^{-1}	349.9 mAh g^{-1}
CoP@AG	377.5 mAh g^{-1}	354.2 mAh g^{-1}

Fig. S12 Galvanostatic charge/discharge profiles and dQ/dV plot of Bare AG and CoP@AG using electrolyte that containing FEC additive.

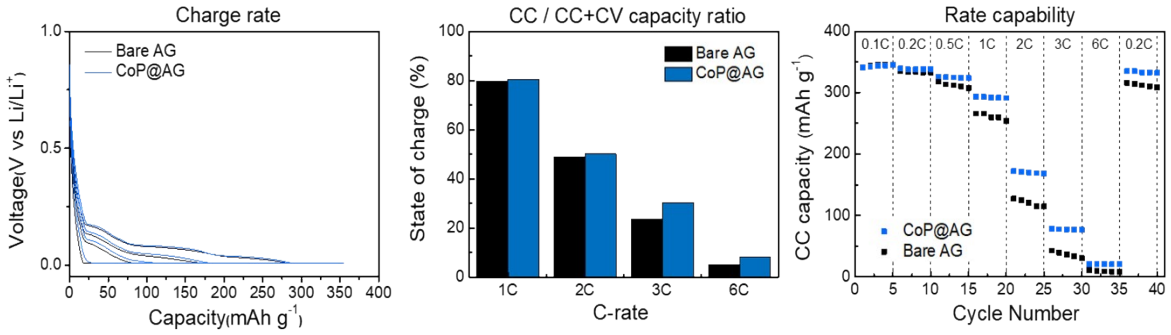

Fig. S13 Rate capability of the Bare AG and CoP@AG half-cell at various C-rates.

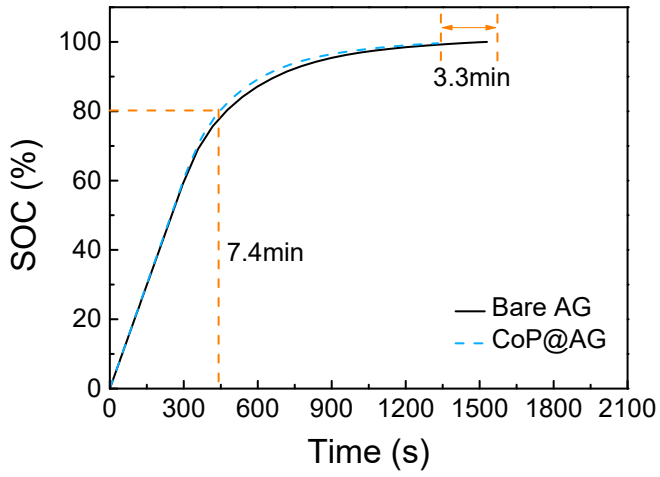

Fig. S14 SOC vs. time profiles of full cells with Bare AG and CoP@AG anodes.

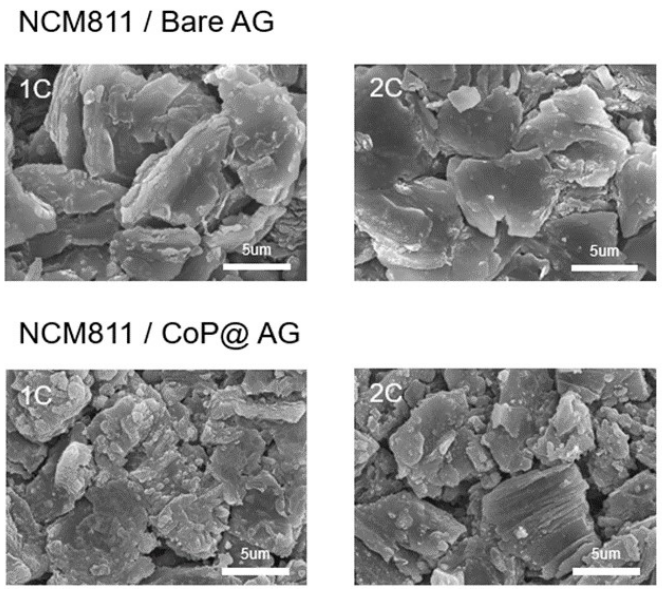

Fig. S15 SEM images of Bare AG and CoP@AG electrodes after 1C, 2C charge.

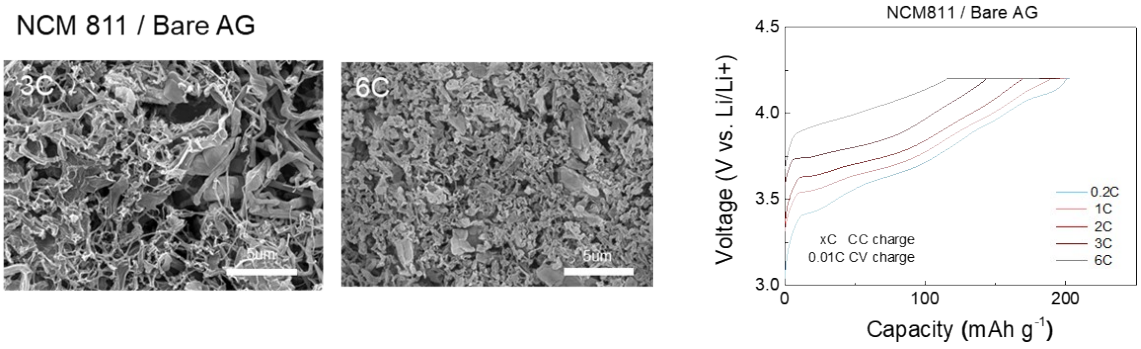

Fig. S16 SEM images of Bare AG electrodes after 3C,6C charge and voltage profile of NCM811 / Bare AG full cell at various C rates.

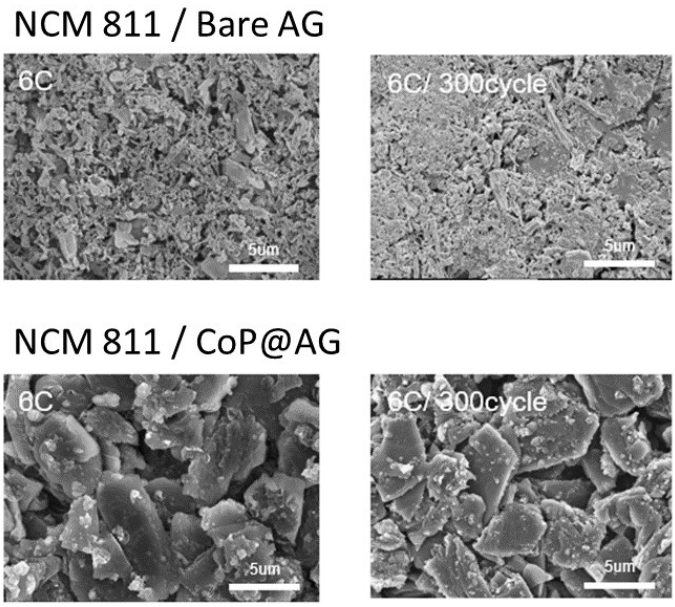

Fig. S17 SEM images of Bare AG and CoP@AG electrodes after 300 cycles at 6C.

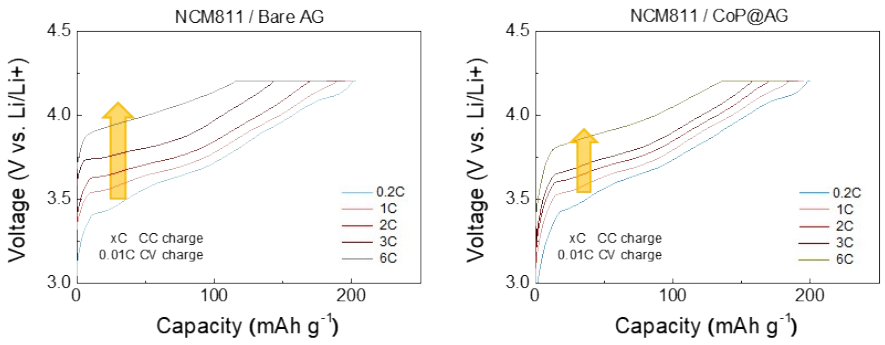

CC/CC+CV(%)	0.2C	1C	2C	3C	6C
Bare AG	98.7%	91.9%	84.1%	71.4%	58.7
CoP@AG	98.7%	93.0%	86.4%	80.6%	68.0

Fig. S18 The CC/CC+CV ratio at each C rate for Bare AG and CoP@AG full cells.

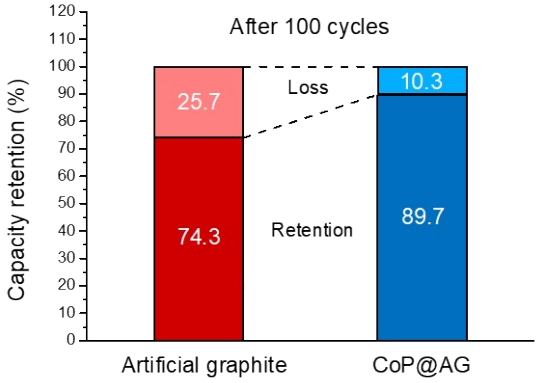

Fig. S19 Capacity retentions of Bare AG and CoP@AG full cells after 100 cycles(6C charging-1C discharging).

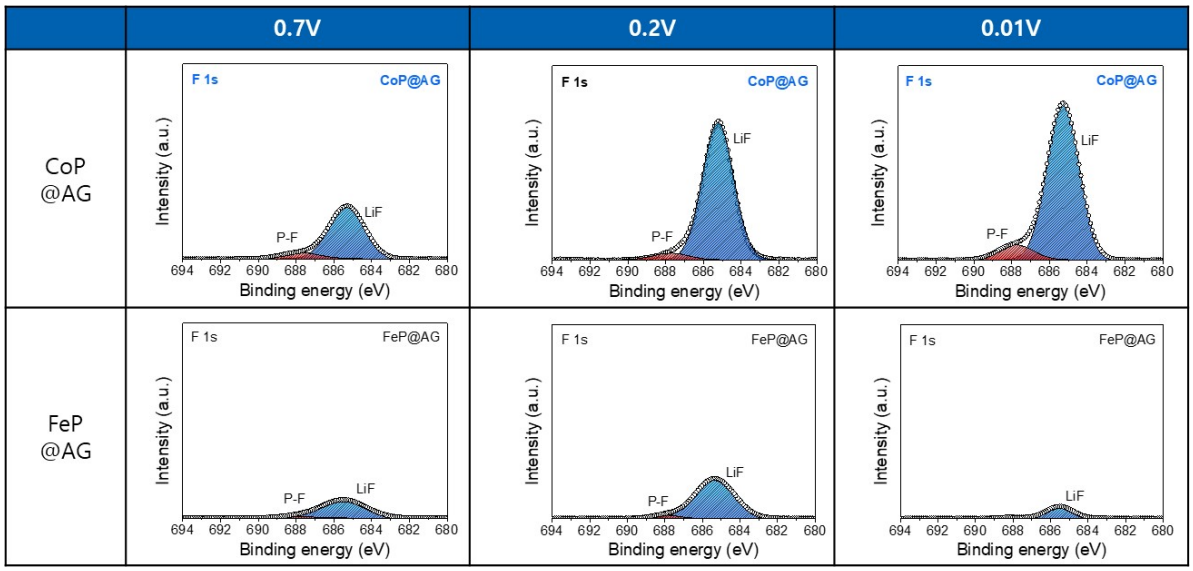

Fig. S20 Evolution behavior of the SEI layer of FeP@AG through XPS analysis after charging to 0.7V, 0.2V and 0.01V.

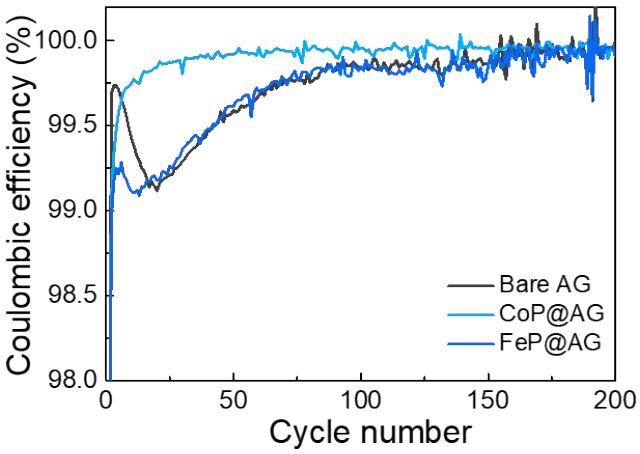

Fig. S21 Coulombic efficiency of Bare AG, CoP@AG and FeP@AG

Example	Electrode composition(wt%) (AM^a : CM^b : BM^c)	N/P ratio	Areal capacity (mAh cm^{-2})	Electrode density (g cm^{-3})	ICE	Fast-charge cyclability (retention) (%cycle no.)	Reference
GPC	92:2:6	1.1	1.5	-	91.1	1C (84%, 200cycle)	1
Gr@$La_{0.1}$TNO	93:2:5	0.6	0.95	-	86.4	3C(76%, 200cycle)	2
Photo-graphite	93:3:4	1.1	2.9	-	94.3	3C(95%, 50cycle)	3
Graphite	80:10:10	1	0.3	-	-	4C(86%,100 cycle)	4
G@Cu-CuNW	94:4:2	1.05	3.2	1.5	91	3C(50%,50c ycle)	5
Edge-plane activated graphite(EAG)	96:1:3	1.1	3.34	1.6	93.8	3C(70%,50c ycle)	6
Mo-CP/graphite	96:0:4	1.1	2.2	1.5	92	6C(84%,300 cycle)	7
CoP@AG (This work)	97.5:1:1.5	1.1	2.2	1.5	91	6C(88%,300 cycle)	This work

a. Active material, b. Conductive agent, c. Binder material

Supplementary Table 1. Comparison of the fast chargeability of various anode materials for

LIBs

Supplementary References

1. M. H. Kim, J. Kim, S. H. Choi, T. U. Wi, A. Choi, J. Seo, C. H. Lim, C. Park and H. W. Lee, *Acs Energy Lett*, 2023, **8**, 3962-3970.
2. Y. L. Sheng, X. Y. Yue, W. Hao, Y. T. Dong, Y. K. Liu and Z. Liang, *Nano Lett*, 2024, **24**, 3694-3701.
3. M. Baek, J. Kim, J. Jin and J. W. Choi, *Nat Commun*, 2021, **12**.
4. C. C. Sun, X. Ji, S. T. Weng, R. H. Li, X. T. Huang, C. N. Zhu, X. Z. Xiao, T. Deng, L. W. Fan, L. X. Chen, X. F. Wang, C. S. Wang and X. L. Fan, *Adv Mater*, 2022, **34**.
5. L. L. Lu, Y. Y. Lu, Z. X. Zhu, J. X. Shao, H. B. Yao, S. G. Wang, T. W. Zhang, Y. Ni, X. X. Wang and S. H. Yu, *Sci Adv*, 2022, **8**.
6. N. Kim, S. Chae, J. Ma, M. Ko and J. Cho, *Nat Commun*, 2017, **8**.
7. S. M. Lee, J. Kim, J. Moon, K. N. Jung, J. H. Kim, G. J. Park, J. H. Choi, D. Y. Rhee, J. S. Kim, J. W. Lee and M. S. Park, *Nat Commun*, 2021, **12**.